Subject- and Resource-Specific Monitoring and Proactive Management of Parallel RF Transmission

Cem Murat Deniz[1,2], Leeor Alon[1,2], Ryan Brown[1], Daniel K. Sodickson[1,2], and Yudong Zhu[1,2]

[1]*Department of Radiology, Bernard and Irene Schwartz Center for Biomedical Imaging, New York University School of Medicine, New York, NY, United States,* [2]*Sackler Institute of Graduate Biomedical Sciences, New York University School of Medicine, New York, NY, United States*

INTRODUCTION: When applying parallel RF transmission in practice, coupling and interaction taking place in the multi-port coil structure and in the subject can significantly affect individual channel RF power delivered towards and reflected from the subject, posing challenges to transmit channel instrumentation and safety monitoring. Tracking these effects and proactively managing the hardware resource in power transmission is important for ensuring a successful scan. By extending subject-specific global SAR calibration and prediction[1,2], a clinically applicable capability of modeling and *predicting* individual channel forward and reflected power *for any RF excitation* became available for the first time[3]. In this study, the forward and reflected power predictions are used proactively to design constrained parallel RF excitation pulses that address the hardware-specific RF power constraints. The constrained parallel RF excitation pulses designed in this way were played out on the MR scanner, and resulting forward and reflected power measurements as well as excitation fidelity are compared with unconstrained pulse designs and designs constrained by global SAR only.

METHODS: Individual channel forward, $P^{(l)}_{fwd}$, and reflected, $P^{(l)}_{rfl}$, power measurements during application of a set of calibration RF pulses[3], $\mathbf{w}_q$, were used to estimate the forward, $\mathbf{\Phi}^{(l)}_{fwd}$, and reflected, $\mathbf{\Phi}^{(l)}_{rfl}$, power correlation matrices of all L channels in addition to the global power correlation matrix $\mathbf{\Phi}$ (Eq. 1). The calibration of forward and reflected power correlation matrices enables the prediction of an individual channel's forward and reflected power at any time instant given an arbitrary set of parallel RF pulses[3]. This property enables proactive power transmission / resource management through RF pulse calculation.

Power Calibration (Eq.1)

Individual Channel: $P^{(l)}_{fwd}=\mathbf{w}_q{}^{H}\mathbf{\Phi}^{(l)}_{fwd}\mathbf{w}_q$

$P^{(l)}_{rfl}=\mathbf{w}_q{}^{H}\mathbf{\Phi}^{(l)}_{rfl}\mathbf{w}_q$

Global: $\sum_l P^{(l)}_{fwd} - \sum_l P^{(l)}_{rfl} = \mathbf{w}_q{}^{H}\mathbf{\Phi}\mathbf{w}_q$

RF Pulse Optimization (Eq. 2)

$$\mathbf{b}^{-}_{full}=\arg\min\|\mathbf{A}_{full}\mathbf{b}_{full}-\mathbf{m}_{des}\|^2$$

such that $\mathbf{b}_{full}{}^{H}\mathbf{\Phi}_{full}\mathbf{b}_{full} \le$ global SAR Limit

$\mathbf{b}_{p\Delta t}{}^{H}\mathbf{\Phi}^{(l)}_{fwd}\mathbf{b}_{p\Delta t} \le P^{(l)}_{fwd,peak}$ *for all l,p*

$\mathbf{b}_{p\Delta t}{}^{H}\mathbf{\Phi}^{(l)}_{rfl}\mathbf{b}_{p\Delta t} \le P^{(l)}_{rfl,peak}$ *for all l,p*

$\alpha\sum_p \mathbf{b}_{p\Delta t}{}^{H}\mathbf{\Phi}^{(l)}_{fwd}\mathbf{b}_{p\Delta t} \le P^{(l)}_{fwd,ave}$ *for all l*

$\alpha\sum_p \mathbf{b}_{p\Delta t}{}^{H}\mathbf{\Phi}^{(l)}_{rfl}\mathbf{b}_{p\Delta t} \le P^{(l)}_{rfl,ave}$ *for all l*

To demonstrate the subject-specific management capacity, individual channel power correlation matrices were incorporated into a parallel transmission RF pulse design by using the convex inequalities as constraints (Eq. 2), where $\mathbf{b}_{p\Delta t}=[b^{(1)}_{p\Delta t} \dots b^{(L)}_{p\Delta t}]^T$ defines the RF pulse weights from L transmit channels at time $p\Delta t$, $P^{(l)}_{fwd,peak}$ represents the lth channel's peak power delivery capacity, $P^{(l)}_{rfl,peak}$ represents the lth channel's tolerance to reflected peak power, $P^{(l)}_{fwd,ave}$ represents the lth channel's average power delivery capacity, $P^{(l)}_{rfl,ave}$ represents the lth channel's average power reflection handling capacity and α = 1 / RF pulse width. In addition to the constraints involving individual power predictions, predefined maximum global SAR limits allowed by FDA guidelines were incorporated using the global power correlation matrix $\mathbf{\Phi}$.

Eq. 2 can be solved by using a range of efficient strategies for convex optimization since the power correlation matrices are positive definite and the constraints are quadratic convex functions. The complexity of the optimization problem increases with the RF pulse length, the number of channels, and the spatial sampling. For a prior simulation-based parallel Tx power optimization investigation[4], a least-squares projection strategy[5] was effective reducing the complexity of optimization finding a small number of basis vectors. This same least-squares projection strategy was employed for the optimization problem, using, specifically, Lanczos algorithm with Gram-Schmidt re-orthogonalization steps[6]. The SeDuMi[7] v1.2.1 solver, interfaced with YALMIP[8], was used to solve the reduced basis convex optimization problem.

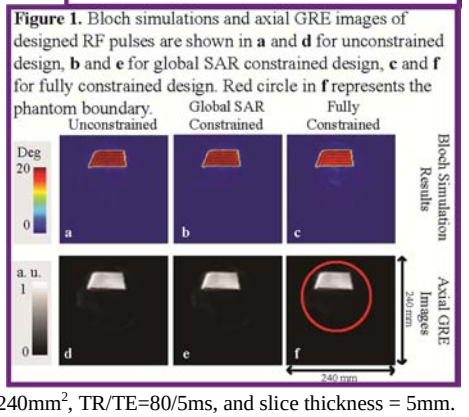

Figure 1. Bloch simulations and axial GRE images of designed RF pulses are shown in **a** and **d** for unconstrained design, **b** and **e** for global SAR constrained design, **c** and **f** for fully constrained design. Red circle in **f** represents the phantom boundary.

Experiments were performed on a whole body 7T scanner (Magnetom, Siemens Medical Solutions) equipped with an 8-channel parallel transmit system (1kW peak power per transmit channel). An 8-channel custom-built stripline coil array was used for RF excitation and reception. Global $\mathbf{\Phi}$, per-channel forward $\mathbf{\Phi}^{(l)}_{fwd}$ and reflected $\mathbf{\Phi}^{(l)}_{rfl}$ power correlation matrices were calibrated using a power sensor (Rhode & Schwarz, NRP-Z11) connected to directional couplers at the output of each RF amplifier. B_1^+ calibration was performed on an axial slice and 20°excitation parallel RF pulses were designed by solving Eq. 2 with no constraints, global SAR constraints, and full constraints (global SAR, peak forward and reflected power, average forward and reflected power). Constant rate spiral-in excitation k-space trajectory was used with duration=4.5ms, excitation resolution=3.8mm, sampling interval=10μs, maximum gradient slew rate=150mT/m/s and gradient amplitude=40mT/m. In the present feasibility study, following power limits were used in constrained RF pulse design: global SAR=3.2W/kg, $P_{fwd,peak}$=700W, $P_{rfl,peak}$=50W, $P_{fwd,ave}$=50W, $P_{rfl,ave}$=25W. Forward and reflected power in 8 channels was measured while calculated RF pulses were used in a GRE acquisition with following parameters: FOV=240x240mm^2, TR/TE=80/5ms, and slice thickness = 5mm.

The capability to predict individual channel forward and reflected power in parallel RF transmission systems can be further leveraged to realize other effects of power management. One example is the minimization of total reflected power, effecting patient-specific matching of the L-channel coil. This was achieved in the present study through RF shimming[9] with virtual coils corresponding to the three smallest eigenvalues of the matrix $\sum_l \mathbf{\Phi}^{(l)}_{rfl}$. Effectiveness of this method was experimentally evaluated.

RESULTS AND DISCUSSION: Axial images resulting from RF pulses designed with various constraints are shown in Fig. 1. The NRMSEs of resultant magnetization from Bloch simulations were 0.0220, 0.0224, and 0.0258 for unconstrained, global SAR constrained, and fully constrained RF pulse designs, respectively. All designs resulted in similar acceptable excitation fidelity. The increase in NRMSE in constrained RF pulse design shows that to meet the strict constraint requirements, some compromise in excitation fidelity was required. However, this 0.3% increase in excitation error is hardly noticeable in the images.

Table 1 summarizes the benefits of RF pulse design under the guidance of calibrated power correlation matrices. RF pulse design without any constraints violated some of the limits in various channels (column Unconstrained). Designing RF pulses with only a global SAR constraint successfully enforced the global SAR limit, but violated peak and reflected power limits in some channels (column Global SAR Constrained). All violations were proactively eliminated by designing the RF pulse with all constraints active (column Fully Constrained). Proper guidance can also be verified by the last column of the Table 1, in which the power prediction matches well with experimental measurements in the indicated channels.

Figure 2 shows, using Channel 4 as an example, predictions and actual measurements of reflected RF power. There is an excellent agreement between power predictions (Fig. 2b) and actual measurements (Fig. 2a). In contrast, calibration of individual channels with the conventional single channel power calibration method (which does not capture contributions to a channel's power transmission by other parallel channels) would lead to predictions equivalent to using power correlation matrices that are without off-diagonal entries -- in the Channel 4 example, thus obtained reflected power predictions (Fig.2c) deviate significantly from actual reflected power measurements, as indicated by red arrows in Fig.2a, and underestimate maximum reflected power. Full power correlation matrix calibrations are necessary for proactive, accurate management of parallel RF transmission.

Table 1. Power comparison of RF pulses with different power constraints.

	Measured			Estimated
	Unconstrained	Global SAR Constrained	Fully Constrained	Fully Constrained
Global SAR (W/kg)	5.14	2.93	2.3	2.4
FWD Peak (W)	1103.2 *(ch3)*	916.2 *(ch1)*	683.9 *(ch4)*	700
RFL Peak (W)	86.5 *(ch3)*	67.5 *(ch3)*	46.4 *(ch3)*	50
FWD Average (W)	65.3 *(ch1)*	40.3 *(ch1)*	30.7 *(ch1)*	33.5
RFL Average (W)	3.7 *(ch2)*	2.2 *(ch3)*	1.59 *(ch3)*	1.96

Compared to use of all 8 coil elements, using three synthesized virtual coil elements to improve, actively, patient - specific coil matching decreased reflected / forward power ratio from 8.1% to 1.7% while slightly increased the B_{1+} nonuniformity (defined as standard deviation over mean) from 0.29 to 0.31.

In addition to the global SAR limits, local SAR limits, obtained via FDTD simulations[10] or experimental calibration[11], can also be included into the constrained optimization problem (Eq. 2) as additional constraints for ensuring patient safety. However, the most challenging part in proactive local SAR management appears to be accurate local SAR prediction models[12].

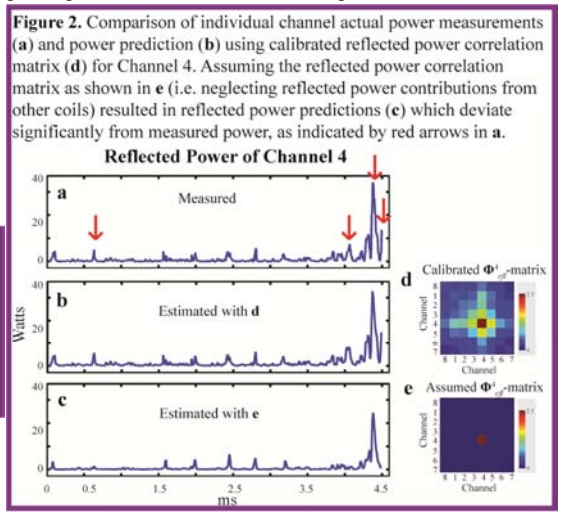

Figure 2. Comparison of individual channel actual power measurements (**a**) and power prediction (**b**) using calibrated reflected power correlation matrix (**d**) for Channel 4. Assuming the reflected power correlation matrix as shown in **e** (i.e. neglecting reflected power contributions from other coils) resulted in reflected power predictions (**c**) which deviate significantly from measured power, as indicated by red arrows in **a**.

REFERENCES: [1] Zhu Y. (2009) ISMRM: 2585. [2] Alon L, et al. (2010): ISMRM 780. [3] Zhu Y, et al. (2012) MRM 67: 1367-78. [4] Brunner DO, et al. (2010) MRM 63: 1280-91. [5] Hanke M. (2001) BIT Numerical Mathematics 41:1008-18. [6] Golub GH, et al. (1996) JHU Press: Matrix Computations. [7] Sturm, JF (1997) PhD Thesis, Tilburg University. [8] Lofberg, J. (2004) CACSD: 284-289. [9] Hoult DI. (2000) JMRI 12: 46-67. [10] Collins CM, et al. (1998) MRM 40: 847-56. [11] Alon L, et al. (2012) MRM doi: 10.1002/mrm.24374. [12] Homann H, et al. (2011) MRM 66: 1767-76.